Filomat 37:6 (2023), 1701–1712
https://doi.org/10.2298/FIL2306701V

Published by Faculty of Sciences and Mathematics,
University of Niš, Serbia
Available at: http://www.pmf.ni.ac.rs/filomat

Visualization of spheres in the generalized Hahn space

Vesna I. Veličković[a], Edin Dolićanin[b]

[a] *Department of Computer Science, Faculty of Sciences and Mathematics, University of Niš, Niš, Serbia*
[b] *Department of Technical Science, State University of Novi Pazar, Serbia*

Abstract. We introduce the generalized Hahn space $h_d(p)$, which is not normable, and show that it is a totally paranormed space. We develop the parametric representation of parts of spheres in three–dimensional space endowed with the relative paranorm of $h_d(p)$ and solve the visibility and contour problems for these spheres. Also we apply our own software in line graphics to visualize the shapes of parts of these spheres. Finally we demonstrate the effects of the change of the parameters d and p on the shape of the spheres.

1. Introduction and Background

Visualization is widely used in teaching and research as useful tools for better understanding mathematical concepts and results. It is also frequently applied in natural and engineering sciences.

Here we use our own software in line graphics to visualize the geometry of linear metric spaces that have recently been used and studied in functional analysis and operator theory. This goal is achieved by graphically representing spheres in the metric of the studied spaces.

We introduce the generalized Hahn space $h_d(p)$, prove that it is a linear metric space with respect to its natural total paranorm, and solve the visibility and contour problems for the visualization of spheres or their parts in $h_d(p)$.

Finally we demonstrate the influence of the change of the parameters p and d on the shapes of the spheres in $h_d(p)$.

We use the standard notations ω for the set of all complex sequences $x = (x_k)_{k=1}^{\infty}$, and c_0 for the set of all sequences in ω that converge to zero.

The Hahn space h was originally introduced and studied by Hahn in 1922 [5] in connection with the theory of singular integrals, and later generalized to h_d by Goes [4] for sequences $d = (d_k)_{k=1}^{\infty}$ of positive reals, where

$$h_d = \{x \in \omega : \sum_{k=1}^{\infty} d_k|\Delta x_k| < \infty\} \cap c_0,$$

and $\Delta x_k = x_k - x_{k+1}$ for all k. In the special cases, where $d_k = k$ or $d_k = 1$ for all k, the generalized Hahn space reduces to the original Hahn space h or the classical space bv_0 (see, for instance, [18, Definition

2020 *Mathematics Subject Classification*. Primary: 68U07; Secondary: 46–04, 46A45.
Keywords. Visualizations; Shapes of spheres; Generalized Hahn sequence space; Visibility and contour.
Received: 06 February 2022; Accepted: 20 February 2022
Communicated by Vladimir Rakočević
Email addresses: vesna@pmf.ni.ac.rs (Vesna I. Veličković), edin@np.ac.rs (Edin Dolićanin)

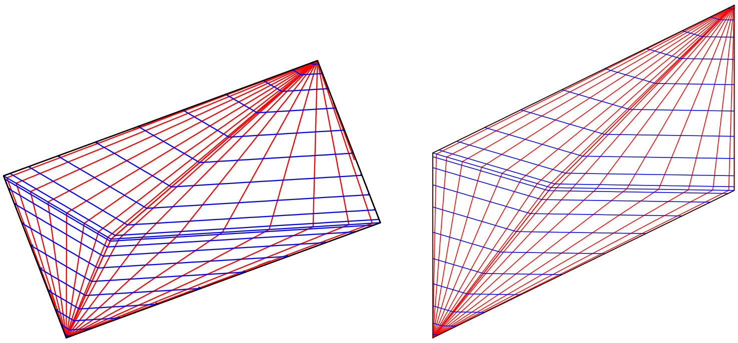

Figure 1: Left: Sphere in the original Hahn space. Right: Sphere in the bv_0 space

7.3.3]), respectively (Figure1). It was shown in [13, Proposition 2.1] that if the sequence d is increasing and unbounded, then h_d is a BK space with AK (see, for instance, [12, Definitions 9.2.1 and 9.2.12] for the concepts of BK space and AK).

Matrix transformations and bounded and compact operators on the Hahn space have recently been studied in various papers, for instance in [1, 2, 7, 9, 10, 13–16]. A survey of recent results can also be found in [6].

We generalize the definition of the space h_d.
Let $(p_k)_{k=1}^\infty$ be a sequence of positive real numbers and $d = (d_k)_{k=1}^\infty$ be an increasing unbounded sequence of positive real numbers. We write [8]

$$c_0(p) = \left\{x = (x_k)_{k=1}^\infty \in \omega : \lim_{k\to\infty} |x_k|^{p_k} = 0\right\},$$

and define the set

$$h_d(p) = \left\{x = (x_k)_{k=1}^\infty \in \omega : \sum_{k=1}^{\infty} d_k \, |\Delta x_k|^{p_k} < \infty\right\} \cap c_0(p).$$

If $d_k = k$ for all k, then we write $h(p) = h_d(p)$.

2. The Generalized Paranormed Hahn Space

Throughout, let $(p_k)_{k=1}^\infty$ be a sequence of positive real numbers and $d = (d_k)_{k=1}^\infty$ be an increasing unbounded sequence of positive reals. In this section, we show that the space $h_d(p)$ is a totally paranormed space, if the sequence p is bounded.

We recall the concept of a *paranorm* (see, for instance, [17, Definition 4.2.1]).

Definition 2.1. Let X be a linear space.
A function $g : X \to \mathbb{R}$ is called a *paranorm*, if

$$g(0) = 0, \tag{P.1}$$
$$g(x) \geq 0 \text{ for all } x \in X, \tag{P.2}$$
$$g(-x) = g(x) \text{ for all } x \in X, \tag{P.3}$$
$$g(x + y) \leq g(x) + g(y) \text{ for all } x, y \in X \text{ (\textit{triangle inequality})} \tag{P.4}$$
$$\begin{array}{l}\text{if } (\lambda_n) \text{ is a sequence of scalars with } \lambda_n \to \lambda \ (n \to \infty) \text{ and } (x_n) \text{ is a} \\ \text{sequence of vectors with } g(x_n - x) \to 0 \ (n \to \infty) \text{ then it follows that} \\ g(\lambda_n x_n - \lambda x) \to 0 \ (n \to \infty) \text{ (\textit{continuity of multiplication by scalars}).}\end{array} \tag{P.5}$$

If g is a paranorm on X, then (X, g), or X for short, is called a *paranormed space*. A paranorm g for which $g(x) = 0$ implies $x = 0$ is called *total*.

Remark 2.2. If g is a total paranorm for a linear space X, then it is easy to see that $d(x, y) = g(x-y)$ $(x, y \in X)$ defines a metric on X, which is translation invariant, thus every totally paranormed space is a translation invariant linear space. The converse statement is also true. The metric of any linear metric space is given by some total paranorm [17, Theorem 10.4.2].

The following holds.

Proposition 2.3. *If the sequence $p = (p_k)_{k=1}^{\infty}$ is bounded, then $(h_d(p), g_{(p)})$ is a totally paranormed space with*

$$g_{(p)}(x) = \left(\sum_{k=1}^{\infty} d_k\, |\Delta x_k|^{p_k}\right)^{1/M} \quad (x \in h_d(p)),$$

where $M = \max\{1, \sup_k p_k\}$.

Proof. (i) First we show that $h_d(p)$ is a linear space.
We write $\alpha_k = p_k/M$ and $\delta_k = d_k^{1/p_k}$ for all k.
Let $x, y \in h_d(p)$. Then $x, y \in c_0(p)$ and so, since $\alpha_k \leq 1$ for all k

$$|x_k + y_k|^{\alpha_k} \leq |x_k|^{\alpha_k} + |y_k|^{\alpha_k} \to 0 \ (k \to \infty),$$

hence $x + y \in c_0(p)$. Also we get applying Minkowski's inequality

$$\begin{aligned}
\left(\sum_{k=1}^{\infty} d_k \left|\Delta(x+y)_k\right|^{p_k}\right)^{1/M} &= \left(\sum_{k=1}^{\infty} \left(\left|\delta_k \Delta x_k + \delta_k \Delta y_k\right|^{\alpha_k}\right)^{M}\right)^{1/M} \\
&\leq \left(\sum_{k=1}^{\infty} |\delta_k \Delta x_k|^{\alpha_k M}\right)^{1/M} + \left(\sum_{k=1}^{\infty} \left|\delta_k \Delta y_k\right|^{\alpha_k M}\right)^{1/M} \\
&= \left(\sum_{k=1}^{\infty} d_k |\Delta x_k|^{p_k}\right)^{1/M} + \left(\sum_{k=1}^{\infty} d_k |\Delta y_k|^{p_k}\right)^{1/M} < \infty. \qquad (1)
\end{aligned}$$

Thus we have shown that $x, y \in h_d(p)$ implies $x + y \in h_d(p)$.
Now we assume $x \in h_d(p)$ and $\lambda \in \mathbb{C}$. We put $\Lambda = \max\{1, |\lambda|^M\}$ and obtain from $x \in c_0(p)$

$$|\lambda x_k|^{p_k} \leq \Lambda |x_k|^{p_k} \to 0 \ (k \to \infty)$$

that $\lambda x \in c_0(p)$, and also

$$\sum_{k=1}^{\infty} d_k\, |\lambda \Delta x_k|^{p_k} \leq \Lambda \sum_{k=1}^{\infty} d_k\, |\Delta x_k|^{p_k} < \infty,$$

hence $\lambda x \in h_d(p)$. This completes Part (i) of the proof.
(ii) Now we show that $g_{(p)}$ is a total paranorm on $h_d(p)$.
We write $g = g_{(p)}$, for short.
Obviously $g : h_d(p) \to \mathbb{R}$ satisfies the conditions in (P.1), (P.2) and (P.3), and by (1) also the condition in (P.4) of Definition 2.1.
To show the condition in (P.5) of Definition 2.1 we assume that $(\lambda_n)_{n=1}^{\infty}$ is a sequence of scalars with $\lambda_n \to \lambda$ $(n \to \infty)$ and $(x^{(n)})_{n=1}^{\infty}$ is a sequence of elements $x^{(n)} = (x_k^{(n)})_{k=1}^{\infty}$ in $h_d(p)$ with $g(x^{(n)} - x) \to 0$ $(n \to \infty)$. It follows that

$$g\left(\lambda_n x^{(n)} - \lambda x\right) = S_{1;n} + S_{2;n} + S_{3;n}, \qquad (2)$$

where

$$S_{1;n} = g\left((\lambda_n - \lambda)(x^{(n)} - x)\right),\ S_{2;n} = g\left(\lambda(x^{(n)} - x)\right) \text{ and } S_{3;n} = g\left((\lambda_n - \lambda)x\right).$$

First, $\lambda_n \to \lambda$ $(n \to \infty)$ implies $|\lambda_n - \lambda| \leq 1$ for all sufficiently large n, hence

$$S_{1;n} \leq g\left(x^{(n)} - x\right) \to 0 \ (n \to \infty).$$

We also have

$$S_{2;n} \leq \Lambda g\left(x^{(n)} - x\right) \to 0 \ (n \to \infty).$$

Finally, to show $S_{3;n} \to 0$ $(n \to \infty)$, let $\varepsilon > 0$ be given. Then there exists $k_0 \in \mathbb{N}$ such that

$$\left(\sum_{k=k_0+1}^{\infty} d_k|\Delta x_k|^{p_k}\right)^{1/M} < \frac{\varepsilon}{2}.$$

Now we choose $n_0 \in \mathbb{N}$ such that

$$|\lambda_n - \lambda| \leq 1 \text{ and } \max_{1\leq k\leq k_0} |\lambda_n - \lambda|^{p_k} \leq \left(\frac{\varepsilon}{2g(x)+1}\right)^M \text{ for all } n \geq n_0.$$

Since $1/M \leq 1$, we obtain for all $n \geq n_0$

$$\begin{aligned} S_{3;n} &= \left(\sum_{k=1}^{\infty} |\lambda_n - \lambda|^{p_k} d_k|\Delta x_k|^{p_k}\right)^{1/M} \\ &\leq \left(\sum_{k=1}^{k_0} |\lambda_n - \lambda|^{p_k} d_k|\Delta x_k|^{p_k}\right)^{1/M} + \left(\sum_{k=k_0+1}^{\infty} |\lambda_n - \lambda|^{p_k} d_k|\Delta x_k|^{p_k}\right)^{1/M} \\ &\leq \frac{\varepsilon}{2g(x)+1} \cdot \left(\sum_{k=1}^{\infty} d_k|\Delta x_k|^{p_k}\right)^{1/M} + \left(\sum_{k=k_0+1}^{\infty} d_k|\Delta x_k|^{p_k}\right)^{1/M} \\ &< \frac{\varepsilon}{2} + \frac{\varepsilon}{2} = \varepsilon. \end{aligned}$$

Hence we also have $S_{3;n} \to 0$ $(n \to \infty)$ and consequently the condition in (P.5) of Definition 2.1 is satisfied. □

Remark 2.4. Only $d_k > 0$ for all k is needed in the proof of Proposition 2.3.

The following example shows that $h_d(p)$ may not be a linear space if the sequence p is unbounded.

Example 2.5. If the sequence p is unbounded and increasing, then the set $h(p)$ is not a linear space.

Proof. We assume that $\sup_k p_k = \infty$. Then we can choose a sequence $(k(i))_{i=1}^{\infty}$ of integers such that $k(i) > i + 1$ and $k(i+1) - k(i) > 2$ for all i. We define the sequence $x = (x_k)_{k=1}^{\infty}$ by

$$x_k = \begin{cases} \dfrac{1}{2}\left(\dfrac{1}{k(i)}\right)^{1/p_{k(i)-1}} & (k = k(i)) \\ 0 & (k \neq k(i)) \end{cases} \quad (i = 1, 2, \dots).$$

Then it follows that

$$\sum_{k=1}^{\infty} k|\Delta x_k|^{p_k} = \sum_{i=1}^{\infty} \frac{k(i)-1}{2^{p_{k(i)-1}}} \frac{1}{k(i)} + \sum_{i=1}^{\infty} \frac{k(i)^{1-p_{k(i)}/p_{k(i)-1}}}{2^{p_{k(i)}}}$$

$$\leq \sum_{i=1}^{\infty} \frac{1}{2^i} + \sum_{i=1}^{\infty} \frac{1}{2^{i+1}} < \infty,$$

and, for all k,

$$0 \leq |x_k|^{p_k} \leq \left(\frac{1}{2}\right)^{p_{k(i)}} \frac{1}{k(i)} \to 0 \ (i \to \infty),$$

that is, $x \in h(p)$, but

$$\sum_{k=1}^{\infty} k|2\Delta x_k|^{p_k} \geq \sum_{i=1}^{\infty} \frac{k(i)-1}{k(i)} = \sum_{i=1}^{\infty} \left(1 - \frac{1}{k(i)}\right) = \infty,$$

since $1/k(i) \to 0$ as $i \to \infty$, and so $2x \notin h(p)$. $\square$

3. Visibility and Contour

Let k_1, k_2 and k_3 be distinct positive integers, and the orthogonal projection $pr : \omega \to \mathbb{V}^3$ be defined by $pr(x) = \{x_{k_1}, x_{k_2}, x_{k_3}\}$ for all sequences $x = (x_k)_{k=1}^{\infty} \in \omega$.

In this section, we consider the visualization of the projections pr of parts of spheres in the space $h_d(p)$ on three–dimensional vector space $\mathbb{V}^3$ equipped with the restriction $g_{(p)}\big|_{\mathbb{V}^3}$ of the paranorm $g_{(p)}$ on $\mathbb{V}^3$. Since we use line graphics, perhaps the greatest challenge is solving the visibility problem; we also have to solve the contour (or silhouette) problem.

First we solve the visibility problem.
We use central projection in $\mathbb{V}^3$ and check the visibility of any point on a given surface analytically. This means we have to compute the intersections of straight lines with the surface.

To contract notation, we always write 1, 2 and 3 for the indices k_1, k_2 and k_3 in the computations below. So let d_k and p_k ($k = 1, 2, 3$) be given positive real numbers, $M = \max\{1, p_1, p_2, p_3\}$,

$$g_{(p)}\big|_{\mathbb{V}^3}(\vec{x}) = (d_1|x_1 - x_2|^{p_1} + d_2|x_2 - x_3|^{p_2} + |x_3|^{p_3})^{1/M}$$

for all $\vec{x} = \{x_1, x_2, x_3\} \in \mathbb{V}^3$, and

$$S_r(0) = \{\vec{x} \in \mathbb{V}^3 : g_{(p)}\big|_{\mathbb{V}^3}(\vec{x}) = r\}$$

denote the sphere of radius $r > 0$ centred at the origin. We note that we only need to consider spheres centered at the origin for the solution of the visibility problem, since $g_{(p)}$ is translation invariant by Remark 2.2.

Furthermore, let $\vec{x}(u_1, u_2)$ ($(u_1, u_2) \in R = I_1 \times I_2 \subset (-\pi/2, \pi/2) \times (0, 2\pi)$) be a parametric representation of the part S of the sphere $S_r(0)$ in $(\mathbb{V}^3, g_{(p)}\big|_{\mathbb{V}^3})$ to be visualized (Figure 2), $\vec{q} = \{q_1, q_2, q_3\}, \vec{v} = \{v_1, v_2, v_3\} \in \mathbb{V}^3$ and L be the straight line through the point Q with position vector $\vec{q}$ in the direction of the vector $\vec{v}$, that is, L has a parametric representation

$$\vec{z}(t) = \vec{q} + t\vec{v} \ (t \in \mathbb{R}).$$

We have to find the intersection $L \cap S$, that is, the values of t, u_1 and u_2 for which

$$\vec{x} = \vec{x}(u_1, u_2) = \vec{q} + t\vec{v} \ \text{ for } \ \vec{x}(u_1, u_2) \in S. \tag{3}$$

First we establish a parametric representation for S. We put for $(u_1, u_2) \in R$

$$y_1(u_1, u_2) = r^{M/p_1}\mathrm{sgn}(\cos u_2)\,(\cos u_1|\cos u_2|)^{2/p_1}, \tag{4}$$

$$y_2(u_1, u_2) = r^{M/p_2}\mathrm{sgn}(\sin u_2)\,(\cos u_1|\sin u_2|)^{2/p_2} \tag{5}$$

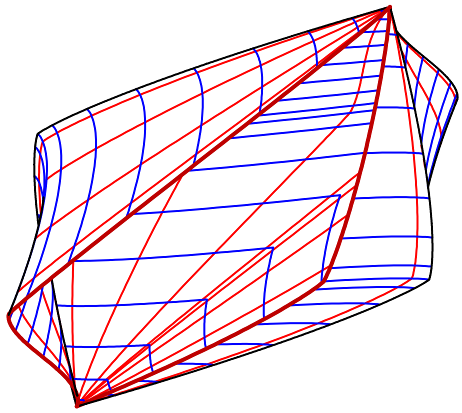

Figure 2: Part of a sphere for $d_1 = 1$, $d_2 = 2$, $d_3 = 3$, $p_1 = 0.8$, $p_2 = 1$, $p_3 = 1.2$.

and

$$y_3(u_1, u_2) = r^{M/p_3}\operatorname{sgn}(\sin u_1)\,|\sin u_1|^{2/p_3}\,. \tag{6}$$

Finally, we write $\delta_k = d_k^{1/p_k}$ for $k = 1, 2, 3$, use the transformation formulae

$$\left\{\begin{array}{lcl} y_1 & = & \delta_1(x_1 - x_2) \\ y_2 & = & \delta_2(x_2 - x_3) \\ y_3 & = & \delta_3 x_3 \end{array}\right\} \quad \text{and} \quad \left\{\begin{array}{lcl} x_1 & = & y_1/\delta_1 + y_2/\delta_2 + y_3/\delta_3 \\ x_2 & = & y_2/\delta_2 + y_3/\delta_3 \\ x_3 & = & y_3/\delta_3 \end{array}\right\}, \tag{7}$$

and obtain

$$\left(g_{(p)}(x)\right)^M = d_1|x_1 - x_2|^{p_1} + d_2|x_2 - x_3|^{p_2} + d_3|x_3|^{p_3} = \sum_{k=1}^{3} |y_k|^{p_k} = r^M. \tag{8}$$

Thus a parametric representation S is given by

$$\vec{x}(u_1, u_2) = \vec{y}(u_1, u_2) \ ((u_1, u_2) \in R),$$

where the vectors $\vec{x}$ and $\vec{y}$ are related by the transformation formulae (7) above.

Now the identity in (3) yields $x_k - (q_k + tv_k) = 0$ for $k = 1, 2, 3$, and in particular

$$v_3 t = x_3 - q_3.$$

Case 1. $v_3 \neq 0$.
Then we have

$$t = t(u_1) = \frac{x_3 - q_3}{v_3} = \frac{y_3/\delta_3 - q_3}{v_3} = \frac{(1/\delta_3)r^{M/p_3}\operatorname{sgn}(\sin u_1)|\sin u_1|^{2/p_3} - q_3}{v_3}, \tag{9}$$

and (3) yields

$$\begin{aligned} x_1 - x_2 &= (q_1 - q_2) + t(v_1 - v_2), \\ x_2 - x_3 &= (q_2 - q_3) + t(v_2 - v_3), \\ x_3 &= q_3 + tv_3. \end{aligned}$$

Thus using the transformation formulae above and (8) we have to find the zeros $u_1^0 \in I_1$ of the function f, where

$$f(u_1) = d_1 \left|(q_1 - q_2) + t(v_1 - v_2)\right|^{p_1} + d_2 \left|(q_2 - q_3) + t(v_2 - v_3)\right|^{p_2} + d_3 \left|q_3 + tv_3\right|^{p_3} - r^M \tag{10}$$

with $t = t(u_1)$ in (9). We use the numerical methods described in detail in [11, Section 6.1]. In almost all cases, however, we apply the bisection method, since it is the fastest one of the implemented methods. We write $t_0 = t(u_1^0)$. Then

$$\begin{aligned}\delta_1 \left(x_1(u_1^0, u_2) - x_2(u_1^0, u_2)\right) = y_1(u_1^0, u_2) &= r^{M/p_1} \operatorname{sgn}(\cos u_2) \left(\cos u_1^0 |\cos u_2|\right)^{2/p_1} \\ &= \delta_1 \left((q_1 - q_2) + t_0(v_1 - v_2)\right)\end{aligned}$$

implies

$$\left|y_1(u_1^0, u_2)\right|^{p_1} = r^M \left(\cos u_1^0 \cos u_2\right)^2 = d_1 \left|(q_1 - q_2) + t_0(v_1 - v_2)\right|^{p_1},$$

and hence

$$\cos u_2 = \pm \frac{1}{\cos u_1^0} \sqrt{\frac{d_1}{r^M}} \cdot \left|(q_1 - q_2) + t_0(v_1 - v_2)\right|^{p_1/2}. \tag{11}$$

Similarly we obtain

$$\sin u_2 = \pm \frac{1}{\cos u_1^0} \sqrt{\frac{d_2}{r^M}} \cdot \left|(q_2 - q_3) + t_0(v_2 - v_3)\right|^{p_2/2}. \tag{12}$$

Finally, we determine the values of $u_2^0 \in I_2$ from (11) and (12) (if they exist), and are able to compute the possible intersections $L \cap S$.

Let C denote the centre of projection. Now a point $Q = (q_1, q_2, q_3) \in S$ with position vector $\vec{q}$ is invisible (with respect to S) if, for $\vec{v} = \overrightarrow{QC}$, there exist a zero $u_1^0 \in I_1$ of the function f in (10) with corresponding $t_0 = t(u_1^0) > 0$ from (9) and $u_2^0 \in I_2$ from (11) and (12).

Case 2. $v_3 = 0$.
Now we have to find the zeros $u_1^0 \in I_1$ of the function f with

$$f(u_1) = x_3 - q_3 = \frac{y_3}{\delta_3} - q_3 = \frac{r^{M/p_3}}{\delta_3} \operatorname{sgn}(\sin u_1) |\sin u_1|^{2/p_3} - q_3,$$

that is,

$$\operatorname{sgn}(\sin u_1) |\sin u_1|^{2/p_3} = \frac{q_3 \delta_3}{r^{M/p_3}}.$$

If $\operatorname{sgn}(\sin u_1) \neq \operatorname{sgn}(q_3)$, then there exists no zero u_1 of $f(u_1)$. Otherwise we obtain

$$|\sin u_1|^2 = \frac{(|q_3|\delta_3)^{p_3}}{r^M},$$

hence

$$\sin u_1 = \pm \sqrt{\frac{|q_3|^{p_3} d_3}{r^M}},$$

which yields

$$u_1^0 = \pm \sin^{-1} \left(\sqrt{\frac{|q_3|^{p_3} d_3}{r^M}} \right),$$

if $|q_3|^{p_3} d_3 \leq r^M$, which is the case if $P \in S$ for $u_1^0 \in I_1$.
Furthermore, we must find the zeros $t_0 = t(u_1^0)$ of

$$g(t) = d_1|(q_1 - q_2) + t(v_1 - v_2)|^{p_1} + d_2|(q_2 - q_3) + t(v_2 - v_3)|^{p_2} + d_3|q_3|^{p_3} - r^M.$$

Now the transformation formulae

$$\delta_1 \left(x_1(u_1^0, u_2) - x_2(u_1^0, u_2) \right) = y_1(u_1^0, u_2) = r^{M/p_1} \mathrm{sgn}(\cos u_2) \left(\cos u_1^0 |\cos u_2| \right)^{2/p_1}$$

and

$$\delta_2 \left(x_2(u_1^0, u_2) - x_3(u_1^0, u_2) \right) = y_2(u_1^0, u_2) = r^{M/p_2} \mathrm{sgn}(\sin u_2) \left(\cos u_1^0 |\sin u_2| \right)^{2/p_2}$$

yield

$$d_1|(q_1 - q_2) + t_0(v - v_2)|^{p_1} = r^M \cos^2 u_1^0 \cos^2 u_2,$$

hence again (11), and similarly (12).
Now the invisibility of a point $Q \in S$ is determined by the same argument as in Case 1.

Now we consider the contour problem. Let P with the position vector $\vec{x}(u_1, u_2)$ be a point of any surface S, and

$$\vec{n}(u_1, u_2) = \vec{x}_1(u_1, u_2) \times \vec{x}_2(u_1, u_2)$$

be the (unnormed) surface normal vector to S at P, where

$$\vec{x}_k(u_1, u_2) = \frac{\partial \vec{x}}{\partial u_k}(u_1, u_2) \text{ for } k = 1, 2.$$

Then we say that P is a contour point of S, if

$$\overrightarrow{PC} \bullet \vec{n}(u_1, u_2) = 0; \tag{13}$$

the set of all contour points is referred to as the contour (or silhouette) of S.

Now let S be a part of the sphere $S_r(0)$ in $h_d(p)$. We put

$$\rho_k = \frac{2r^{M/p_k}}{p_k} \text{ and } \beta_k = \frac{2}{p_k} - 1 \text{ for } k = 1, 2, 3$$

$s_2 =$sgn$(\sin u_2)$ and $c_2 =$sgn$(\cos u_2)$. Then we obtain for $u_1 \neq 0$ and $u_2 \neq \pi/2, \pi, 3\pi/2$

$$\begin{aligned}
&\frac{\partial y_1}{\partial u_1}(u_1, u_2) = -c_2 \rho_1 \sin u_1 (\cos u_1)^{\beta_1} |\cos u_2|^{\beta_1 + 1}, \\
&\frac{\partial y_2}{\partial u_1}(u_1, u_2) = -s_2 \rho_2 \sin u_1 (\cos u_1)^{\beta_2} |\sin u_2|^{\beta_2 + 1}, \\
&\frac{\partial y_3}{\partial u_1}(u_1, u_2) = \rho_3 \cos u_1 |\sin u_1|^{\beta_3}, \\
&\frac{\partial y_1}{\partial u_2}(u_1, u_2) = -\rho_1 \sin u_2 (\cos u_1)^{\beta_1 + 1} |\cos u_2|^{\beta_1}, \\
&\frac{\partial y_2}{\partial u_2}(u_1, u_2) = \rho_2 \cos u_2 (\cos u_1)^{\beta_2 + 1} |\sin u_2|^{\beta_2},
\end{aligned}$$

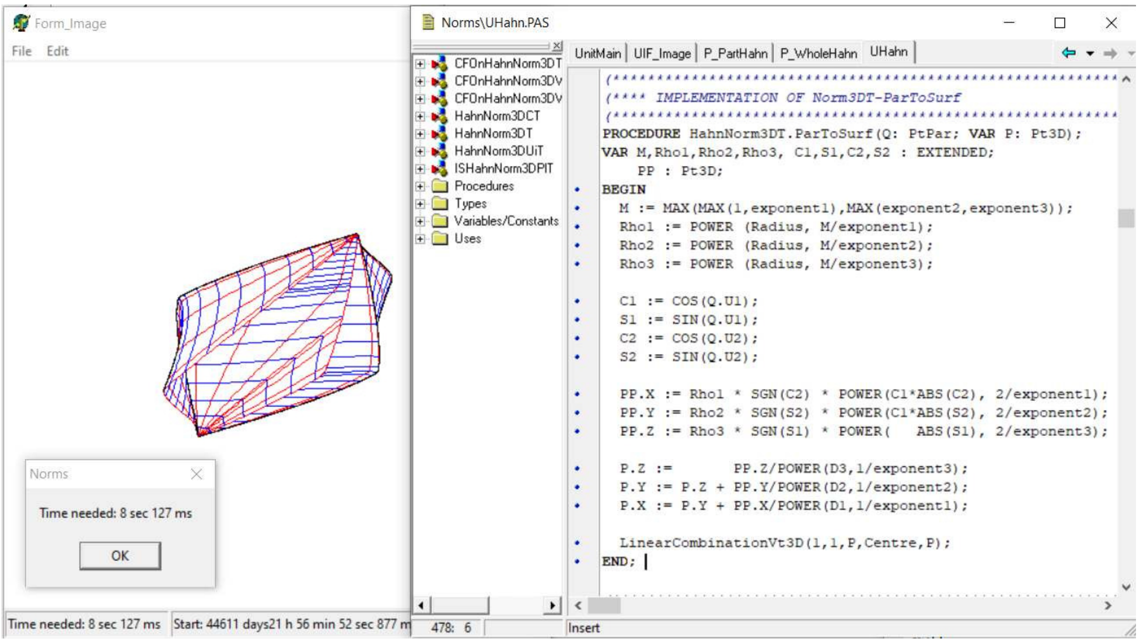

Figure 3: A screenshot for visualization of the sphere in Figure 2 and the implementation of (4) – (7)

and $(\partial y_3/\partial u_2)(u_1, u_2) = 0$. Using the transformation formulae (7) we obtain $\vec{x}_1(u_1, u_2)$ and $\vec{x}_2(u_1, u_2)$.
If $\vec{c}$ denotes the position vector of the centre of projection, then the contour points are given by the zeros in the domain R of S of the function

$$\Phi(u_1, u_2) = (\vec{c} - \vec{x}(u_1, u_2)) \bullet (\vec{x}_1(u_1, u_2) \times \vec{x}_2(u_1, u_2)).$$

For this we use the numerical method to determine the zeros of a real–valued function of two real variables on a rectangle, described in detail in [3].

The described procedure is implemented in our software package *MV-Graphics*. The basics of the software are described in [11]. It contains 135*MB*, and the unit *UHahn* developed for the visualization of spheres in the Hahn space parts of which are described in this paper consists of 1755 lines of programming code. The unit *UHahn* contains, among other things, the classes *HahnNorm*3*DT* for the definition of the spheres in Hahn space, *HahnNorm*3*DUiT* for parameter lines on them and *HahnNorm*3*DCT* for its contour. A screenshot for the visualization of the sphere on the Figure 2 and an implementation of the method *HahnNorm*3*DT*.*ParToSurf* for a given parameter point Q with the resulting three-dimensional point P is given in Figure 3.

A part of the implementation of the visibility procedure described here is

```
M := MAX(MAX(1,exponent1),MAX(exponent2,exponent3));
Vis  := TRUE;  LnIS := PrRay;

LinearCombinationVt3D(1,-1,P,Centre,P);
LinearCombinationVt3D(1,-1,LnIS.O,Centre,LnIS.O);

SpecialCase := Null(LnIS.U.Z,Eps15);

FOR N := 1 TO NOfIntv DO BEGIN
  I1D[1].X := I1[1].X+ (N-1)/NOfIntv*(I1[2].X-I1[1].X);
  I1D[2].X := I1[1].X+     N/NOfIntv*(I1[2].X-I1[1].X);

  FindZerosOfF (I1D, Zero,NoZero);
```

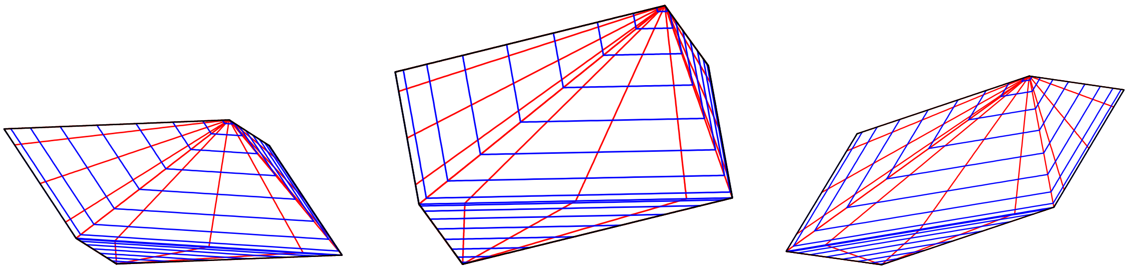

Figure 4: Influence of the parameters d_k

```
    IF (NoZero > 0) THEN BEGIN
      Szero := SIN(Zero);
      Rho3 := POWER (Radius, M/exponent3) / POWER(D3,1/exponent3);
      TT := Rho3 * SGN(Szero) * POWER(ABS(Szero), 2/exponent3) ;

      IF NOT SpecialCase THEN TIS := (TT-LnIS.O.Z)/LnIS.U.Z ELSE TIS := 200;

      IF (TIS > Eps3/DiamWI3D) THEN BEGIN
        Q.U1  := Zero;
        Czero := COS(Zero);
        COSU2 := SQRT(D1) * SGN(LnIS.O.X-LnIS.O.Y + TIS*(LnIS.U.X-LnIS.U.Y))*
                 POWER(ABS(LnIS.O.X-LnIS.O.Y + TIS*(LnIS.U.X-LnIS.U.Y)), exponent1/2) / CZero / POWER(Radius,M/2);
        SINU2 := SQRT(D2) * SGN(LnIS.O.Y-LnIS.O.Z + TIS*(LnIS.U.Y-LnIS.U.Z))*
                 POWER(ABS(LnIS.O.Y-LnIS.O.Z + TIS*(LnIS.U.Y-LnIS.U.Z)), exponent2/2) / CZero / POWER(Radius,M/2);
        COSSINToAngle (COSu2,SINu2, Q.U2);
        IF (Q.U2 < 0) THEN Q.U2 := Q.U2+2*PI;
        IF InIntervalPar (IU1U2,Q) THEN
        BEGIN Vis := FALSE; EXIT; END;
      END;
    END;
  END;
```

4. Influence of Parameters in the Shape of Spheres in $h_d(p)$

We illustrate the influence of each parameter on the shape of the sphere.

Figure 4 illustrates the influence of the parameters d_k. We display the unit spheres with the exponents $p_1 = p_2 = p_3 = 1$. Left: $d_1 = 1, d_2 = 1, d_3 = 3$. Middle: $d_1 = 2, d_2 = 3, d_3 = 5$. Right: $d_1 = 0.5, d_2 = 1.5, d_3 = 2$.

Varying the exponents p_k results in a change of the shape of the spheres. We start with the unit sphere in the original Hahn space h, where $d_1 = 1, d_2 = 2, d_3 = 3$.

First we consider spheres with equal exponents. Figures 5 and 6 show the unit sphere in the generalized Hahn space $h(p)$ with the parameters $p = p_k$ for $k = 1, 2, 3$, where $p = 0.8, 1.3, 2$ and 4.

If the exponents are different, the shape of the sphere is more interesting. On the left in Figure 7, the exponents are $p_1 = 2, p_2 = 4, p_3 = 1$. In the middle, they are $p_1 = 0.8, p_2 = 1, p_3 = 1.2$. In the right they are $p_1 = 2.5, p_2 = 0.8, p_3 = 1.5$. Figure 2 is part of the sphere in the middle.

We can also change the parameters d_k and the exponents p_k at the same time. Figure 8 shows unit spheres in the generalized Hahn space $h_d(p)$. On the left the parameters are $p_1 = 0.5, p_2 = 0.8, p_3 = 1.5$ and $d_1 = 1, d_2 = 1, d_3 = 3$. Notice that the parameters d_k are the same as those on the left in Figure 4. On the right in Figure 8, the parameters are $p_1 = 0.8, p_2 = 1, p_3 = 1.2$ and $d_1 = 0.5, d_2 = 2, d_3 = 4$. The values of p_k are the same as in the middle of Figure 7.

It is also interesting to consider cases where the values of d_k for $k = 1, 2, 3$ are not increasing, since the change of a finite number of terms in the sequence d does not affect the paranorm property of $g_{(p)}$. In Figure 9, the exponents are $p_1 = 2.5, p_2 = 0.8, p_3 = 1.5$, as in right of Figure 7. On the left in Figure 9, the parameters d_k are increasing, $d_1 = 1, d_2 = 3, d_3 = 10$. On the right, they are not monotone, $d_1 = 10, d_2 = 1, d_3 = 3$.

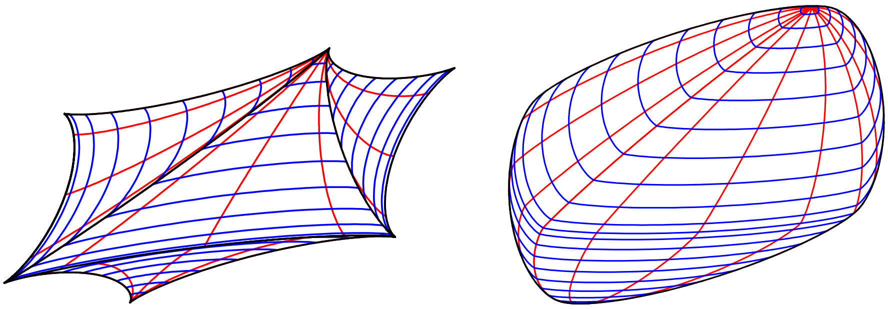

Figure 5: Exponents p_k are equal. Left: $p_k = 0.8$. Right: $p_k = 1.3$

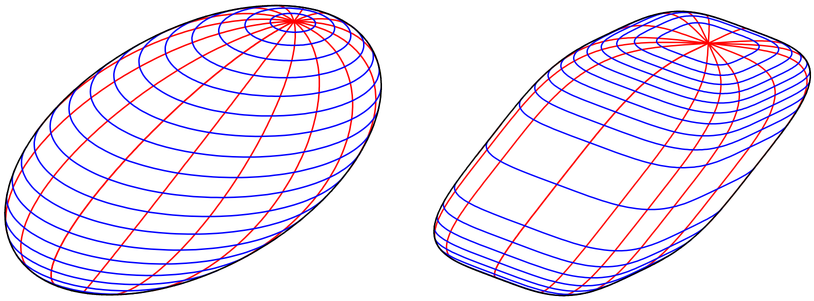

Figure 6: Exponents p_k are equal. Left: $p_k = 2$. Right: $p_k = 4$

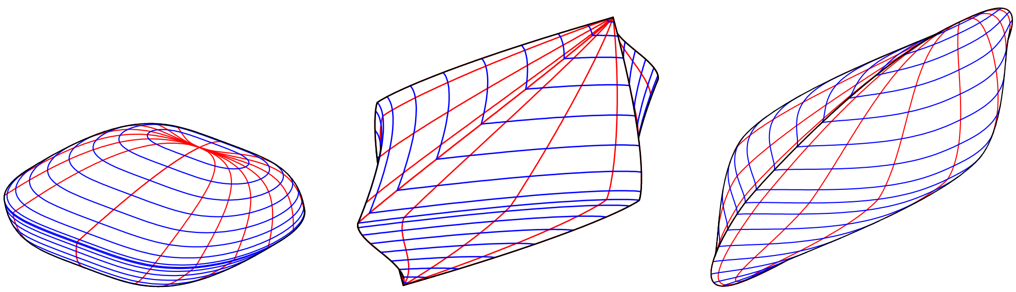

Figure 7: Exponents p_k are different

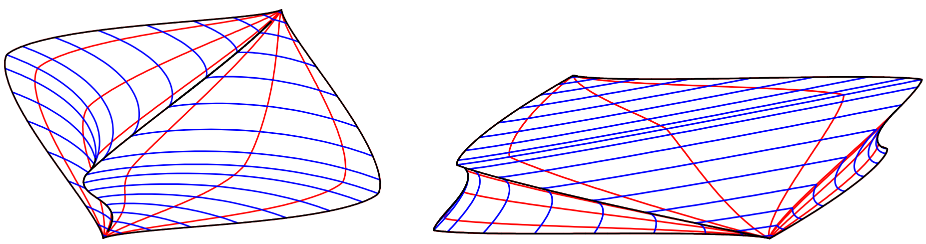

Figure 8: Different parameters d_k and exponents p_k

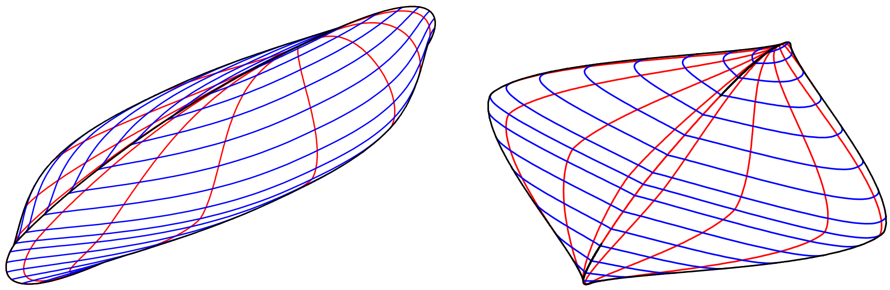

Figure 9: Left: parameters d_k are increasing. Right: parameters d_k are not increasing.

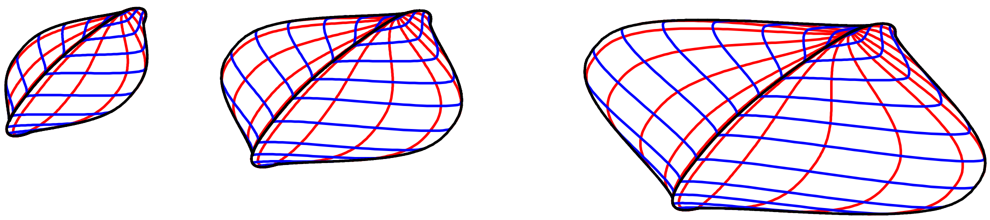

Figure 10: Spheres of radii 1, 1.2 and 1.4.

Finally, we demonstrate the influence of the radius. In Figure 10, we chose the parameters $d_1 = 0.5$, $d_2 = 1$, $d_3 = 1.5$ and for the exponents $p_1 = 1.5$, $p_2 = 0.7$, $p_3 = 2.5$. The radii vary from left to right with the values 1, 1.2 and 1.4 and the centres are on the y–axis at the values 0, 3 and 8. We observe that not only the size is increasing but also it stretches out differently in different dimensions due to the exponents.

References

[1] R. Das. On the fine spectrum of the lower triangular matrix $B(r;s)$ over the Hahn sequence space. *Kyungpook Math. J.*, 57:441–455, 2017.

[2] D. Dolićanin-Djekić and E. Gilić. Characterisations of bounded linear and compact operators on the generalised Hahn space. *Filomat*, 36(2), 2022.

[3] M. Failing and E. Malkowsky. Ein effizientes Nullstellenverfahren zur computergraphischen Darstellung spezieller Kurven und Flächen. *Mitt. Math. Sem. Giessen*, 229:11–28, 1996.

[4] G. Goes. Sequences of bounded variation and sequences of Fourier coefficients II. *J. Math. Anal. Appl.*, 39:477–494, 1972.

[5] H. Hahn. Über Folgen linearer Operationen. *Monatsh. Math. Phys.*, 32:3–88, 1922.

[6] M. Kirişci. The Hahn sequence space defined by the Cesàro mean. *Abstr. Appl. Anal.*, 2013, 2013. Article ID 817659, 6 pages.

[7] M. Kirişci. A survey of the Hahn sequence space. *Gen. Math. Notes*, 19(2):37–58, 2013.

[8] I. J. Maddox. Spaces of strongly summable sequences. *Quarterly J. Math. Oxford*, 18(2):345–355, 1967.

[9] E. Malkowsky. Some compact operators on the Hahn space. *Sci. Res. Comm.*, 1(1):1–14, 2021. doi: 10.52460/src.2021.001.

[10] E. Malkowsky, G. V. Milovanović, V. Rakočević, and et al. The roots of polynomials and the operator Δ_i^3 on the Hahn sequence space h. *Comp. Appl. Math.*, 40(222), 2021. https://doi.org/10.1007/s40314-021-01611-6.

[11] E. Malkowsky and W. Nickel. *Computergrafik in der Differentialgeometrie*. Vieweg Verlag, Braunschweig/Wiesbaden, 1993.

[12] E. Malkowsky and V. Rakočević. *Advanced Functional Analysis*. CRC Press, Taylor & Francis Group, Boca Raton, London, New York, 2019.

[13] E. Malkowsky, V. Rakočević, and O. Tuğ. Compact operators on the Hahn space. *Monatsh. Math.*, 196(3):519–551, 2021.

[14] E. Malkowsky, V. Rakočević, and V. Veličković. Bounded linear and compact operators between the Hahn space and spaces of strongly summable and bounded sequences. *Bull. Sci.Math. Nat. Sci. Math.*, 45:25–41, 2020.

[15] K. Raj and A. Kiliçman. On generalized difference Hahn sequence spaces. *Hindawi Publishing Corporation, The Scientific World Journal Volume 2014*, 2014, 2014. Article ID 398203, 7 pages.

[16] O. Tuğ, V. Rakočević, and E. Malkowsky. Domain of generalized difference operator Δ_i^3 of order three on hahn sequence space h and matrix transformation. *Linear Multilinear Algebra*, 196(3):519–551, 2021.

[17] A. Wilansky. *Functional Analysis*. Blaisdell Publishing Company, New York, Toronto, London, 1964.

[18] A. Wilansky. *Summability through Functional Analysis*, volume 85. North–Holland, Amsterdam, 1984. Mathematical Studies.